

# Thermal Expansion and Elastic Properties of High Gold-Tin Alloys

F.G. YOST, M.M. KARNOWSKY, W.D. DROTNING, and J.H. GIESKE

The Au-Sn eutectic alloy, composed of the  $\zeta$  and  $\delta$  phases, has been used for many years in the sealing of hermetic parts. Recently, it was shown that the  $\zeta$  phase undergoes an ordering transformation to  $\zeta'$ . Since this transformation may affect hermeticity, measurements of density, linear thermal expansion coefficient, elastic moduli, and Poisson's ratio were made on  $\zeta$ -phase, eutectic, and  $\delta$ -phase specimens. Measurements were made over a temperature range that includes the  $\zeta \rightarrow \zeta'$  transformation. Abrupt changes in these thermophysical properties, near the phase transformation temperature, are noted for  $\zeta$  and eutectic specimens but not for the  $\delta$  specimen.

## I. INTRODUCTION

ALLOYS of gold and tin have been used in the semiconductor industry for approximately 30 years.<sup>[1,2,3]</sup> Because of its relatively low eutectic temperature (278 °C), the alloy at 29 at. pct Sn has been most useful for package sealing and die attachment. Until 1974, this alloy was thought to comprise two intermetallic compounds,  $\zeta$  at the approximate stoichiometry Au<sub>5</sub>Sn and  $\delta$  at AuSn. Although there were few apparent problems in using this alloy, Bernstein<sup>[1,2]</sup> reported an unusual dip in the thermal expansion coefficient vs temperature curve. Bernstein was concerned that this dip was caused by phase transformation and that the phenomenon could cause cracking problems. The details of his thermal expansion measurements were not given, but his results are shown in Figure 1, where the dip occurs at approximately 200 °C. He went on to show that a 2 pct substitution of indium for tin resulted in total suppression of this thermal expansion dip.

Giessen<sup>[4]</sup> found considerable metastable phase activity near the  $\zeta$  composition in splat-cooled alloys. He also observed a variant of the  $\zeta$  phase which he referred to as  $\zeta_s$ . Ishihara *et al.*<sup>[5]</sup> used rapid quenching techniques to identify several metastable phases in the Au-Sn system, but it is unlikely that any of those metastable phases could cause problems in the semiconductor industry. In 1974, Osada *et al.*<sup>[6]</sup> discovered that the hexagonal  $\zeta$  phase undergoes an order-disorder phase transformation at approximately 190 °C. The ordered hexagonal phase,  $\zeta'$ , can be seen in the most recent phase diagram for the Au-Sn system.<sup>[7]</sup> It seems clear that the thermal expansion anomaly that concerned Bernstein was due to the  $\zeta \rightarrow \zeta'$  transformation. Since the alloy is often used for sealing electronic packages, this phase transformation may jeopardize hermeticity. This concern indicates that Bernstein's measurements should be confirmed even though the current use of the alloy seems trouble-free. Reported here are measurements of linear thermal expansion coefficients, densities, and elastic moduli. The measurements were made at temperatures ranging from

23 °C to 250 °C on alloys prepared at the  $\zeta$ -phase, eutectic, and  $\delta$ -phase compositions. These findings are interpreted in terms of the current version of the Au-Sn phase diagram.

## II. EXPERIMENT

Three Au-Sn alloys were prepared for the measurement of density, coefficient of linear thermal expansion, elastic moduli (both longitudinal and transverse), and Poisson's ratio. The alloys were prepared with the intention of obtaining the  $\delta$  phase at AuSn, the eutectic composition at 29 at. pct Sn, and the  $\delta'$  phase at Au<sub>5</sub>Sn. High-purity (99.9+) Sn and Au constituents were sealed in 10-mm-diameter quartz flat-bottomed tubes under a vacuum of  $1.3 \cdot 10^{-3}$  Pa. The samples weighing approximately 20 grams each were melted three times, with tube inversion each time to promote homogenization. The  $\delta$  phase was brittle and showed a tendency to crack because of solidification stresses, although two  $\delta$ -phase samples were obtained that appeared free of cracks. All specimens were aged 5 days at 150 °C in quartz tubes before any measurements. The compositions of the alloys were measured by atomic emission spectroscopy, and densities were measured by a hydrostatic weighing method. These data are shown in Table I.

Backscattered electron images of the alloys are shown in Figures 2(a) through (c), and all show various amounts of  $\delta$  and  $\zeta$  phases. The volume fractions of these phases were measured with a TRACOR NORTHERN\* 8502

\*TRACOR NORTHERN is a trademark of Tracor Northern, Inc., Middleton, WI.

Image Analyzer by averaging the readings of five random fields of view. The AuSn specimen, shown in Figure 2(a), has 0.24 vol pct  $\zeta$  phase (light appearing) located at the grain boundaries of the  $\delta$  phase. The presence of the  $\zeta$  phase is in slight disagreement with the chemistry results, which suggest that the alloy should contain a small fraction of  $\epsilon$  phase. The eutectic sample, shown in Figure 2(b), exhibits some  $\zeta$  dendrite formation, which indicates slight departure from the eutectic composition. The volume fraction of the  $\delta$  phase is measured to be 46.3 pct. Figure 2(c) shows a two-phase microstructure in the Au<sub>5</sub>Sn specimen. The minor phase

F.G. YOST, M.M. KARNOWSKY, W.D. DROTNING, and J.H. GIESKE, Technical Staff Members, are with Sandia National Laboratories, Albuquerque, NM 87185.

Manuscript submitted October 13, 1989.

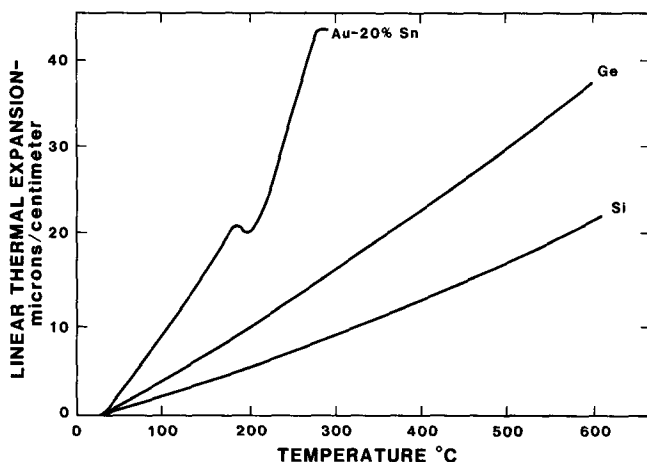


Fig. 1—Thermal expansion behavior of Au-Sn eutectic, obtained by Bernstein,<sup>11,12</sup> showing possible phase transformation near 200 °C.

was identified as AuSn, indicating slight departure from the  $\zeta'$  stoichiometry toward the  $\delta$  phase. This departure is consistent with the chemical analysis. The volume fraction of the  $\delta$  phase is measured to be 7.2 pct. The ordered structure of the  $\zeta'$  phase, in the eutectic and  $\zeta$  alloys, was confirmed by transmission electron microscopy. X-ray analysis was insensitive to the ordering.

Coefficients of thermal expansion were measured using a Harrop fused-silica single-pushrod dilatometer. Calibrations prior to the material tests were made using a National Bureau of Standards-referenced platinum standard. The samples were measured over the range of 23 °C to 250 °C during heating and cooling at 2 °C/min. The data were plotted as linear thermal expansion (LTE) expressed in percent vs temperature. Coefficients of thermal expansion (CTE) were determined over specified temperature ranges by least-squares linear fitting of the data.

The moduli, elastic and shear, were determined by ultrasonic measurements. The mechanical properties of a material with density  $\rho$  are related to the ultrasonic longitudinal velocity,  $V_L$ , and the shear velocity,  $V_S$ , in the material by the following expressions:<sup>18</sup>

$$\text{Lamé constants} \quad \mu = \rho V_S^2 \quad [1]$$

$$\lambda = \rho V_L^2 - 2\rho V_S^2 \quad [2]$$

$$\text{Bulk modulus} \quad B = \lambda + \frac{2}{3}\mu \quad [3]$$

$$\text{Young's modulus} \quad E = \frac{\mu(3\lambda + 2\mu)}{(\lambda + \mu)} \quad [4]$$

$$\text{Shear modulus} \quad G = \mu \quad [5]$$

Table I. Measured Composition and Density of Alloys

Alloy	Au (At. Pct)	Sn (At. Pct)	Density (g/cm <sup>3</sup> )
$\delta$ phase = AuSn	49.9	50.1	11.7
Eutectic	70.8	29.2	14.7
$\zeta'$ phase = Au <sub>5</sub> Sn	82.7	17.3	16.3

$$\text{Poisson's ratio} \quad \nu = \frac{\lambda}{2(\lambda + \mu)} \quad [6]$$

The ultrasonic longitudinal and shear velocities were measured at temperature  $T$  using the technique developed by Gieske and Frost.<sup>19</sup> Two thermocouples were used on the surface of each sample and showed consistency within 2 °C at temperatures <100 °C, 3 °C at 100 °C <  $T$  < 200 °C, and 4 °C at temperatures >200 °C. Approximately 30 minutes dwell time were spent at each measurement temperature. Accurate time delay measurements,  $t_0$ , for the ultrasonic wave to travel through each specimen were made at room temperature by the pulse echo overlap or equivalent through transmission methods. The room-temperature velocity value was then determined by

$$V_0 = L_0/t_0 \quad [7]$$

where  $L_0$  is the length of the specimen. Single velocity measurements were determined with errors <1 pct, giving a moduli error of approximately 2 pct. For the two  $\delta$ -phase specimens, the fastest velocity values were used in the moduli calculations to minimize the effects of small solidification cracks which may have been present. The time delay for the wave to travel through the specimen at temperature  $T$  was compared with the room-temperature reference value,  $t_{\text{ref}}$ , and the difference ( $t - t_{\text{ref}}$ ) was recorded vs temperature.<sup>19</sup> The velocity at a given temperature  $T$  was determined by

$$V(T) = \frac{L(T)}{t(T)} = \frac{L_0(1 + \alpha(T - T_0))}{t_0 + (t - t_{\text{ref}})} \quad [8]$$

where  $\alpha$  is the CTE and  $T_0$  is the room-temperature reference. The density at  $T$  is given by

$$\rho(T) = \rho_0 \cdot (1 + \alpha(T - T_0))^{-3} \quad [9]$$

where  $\rho_0$  is the room-temperature density. The elastic constants and moduli were calculated at the temperature  $T$  using Eqs. [8] and [9] and the corresponding expressions [1] through [6] listed above. Changes in moduli vs temperature were measured to less than 0.5 pct.

### III. RESULTS

#### A. Coefficients of Thermal Expansion

The AuSn alloy was well behaved and exhibited slight upward curvature, as shown in Figure 3. The average CTE for AuSn was found to be  $14.0 \cdot 10^{-6}/^\circ\text{C}$  over the range of 23 °C to 250 °C. The eutectic composition showed some complexity. Below the transition temperature (190 °C), all CTE runs agreed, being  $16.2 \cdot 10^{-6}/^\circ\text{C}$  on heating to  $16.8 \cdot 10^{-6}/^\circ\text{C}$  on cooling. These values were independent of the specimen thermal history during the measurement cycle. The specimen was observed to shrink about 0.05 pct during the 4-day anneal at 250 °C. Following the isothermal anneal, the CTE values above the transition temperature were  $15.6 \cdot 10^{-6}/^\circ\text{C}$  on cooling and  $17.0 \cdot 10^{-6}/^\circ\text{C}$  on heating. Figure 4 illustrates this behavior. The  $\zeta$  phase showed similar behavior and, during the initial heating run, yielded a CTE of  $17.8 \cdot 10^{-6}/^\circ\text{C}$  below the transition temperature and a CTE of

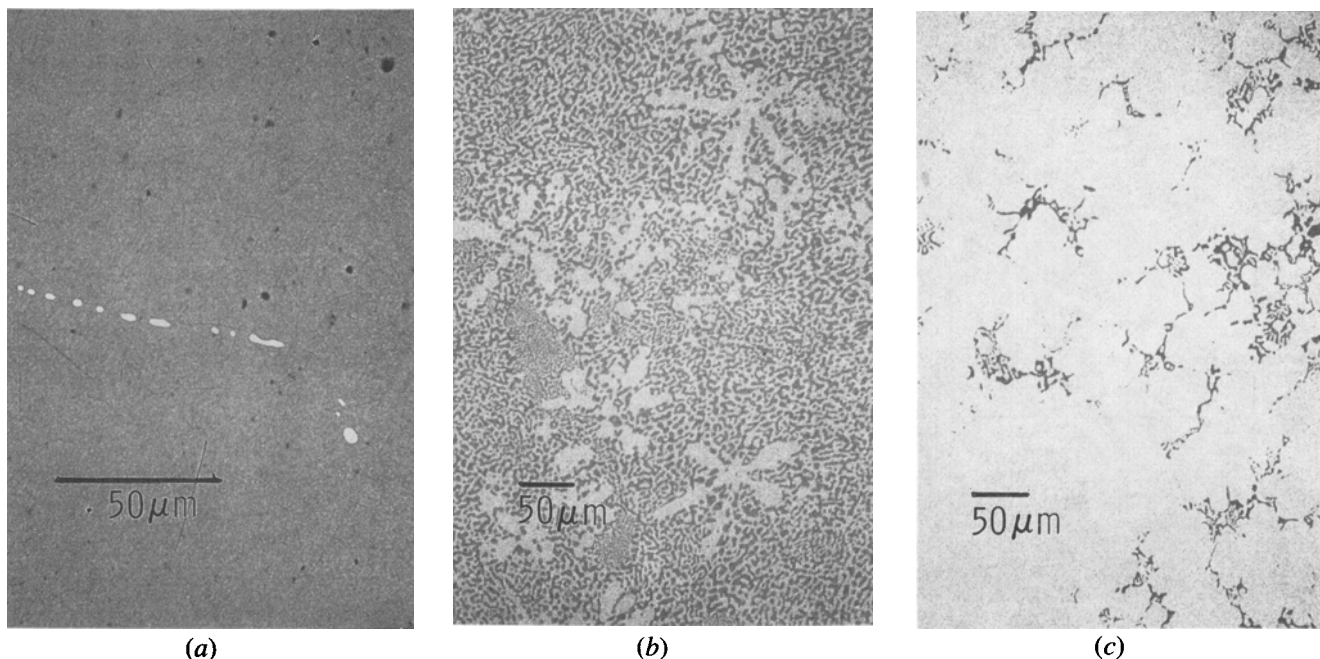


Fig. 2—Backscattered electron image of (a)  $\delta$  phase, showing minor amount of  $\zeta$  phase (light appearing inclusions), (b) eutectic alloy, showing 46.3 pct  $\delta$  phase (dark appearing phase), and (c)  $\zeta$  phase, showing 7.2 pct  $\delta$  phase (dark appearing phase).

$21.2 \cdot 10^{-6}/^{\circ}\text{C}$  above the transition temperature. A subsequent anneal at  $250^{\circ}\text{C}$  for 8 days produced a shrinkage of 0.34 pct, which was confirmed by subsequent measurement at ambient temperature. After this high-temperature anneal, CTEs were found to be  $19.7 \cdot 10^{-6}/^{\circ}\text{C}$  and  $21.0 \cdot 10^{-6}/^{\circ}\text{C}$  below and above the transition temperature. Figure 5 shows these results. The measured differences in CTEs upon heating and cooling are believed significant but subject to experimental error due to thermal lag and irreversible effects of the phase transformation.

### B. Moduli of Elasticity

The ultrasonic velocity measurements yielded the bulk modulus, Young's modulus, shear modulus, and Poisson's

ratio. The fitted equation for the moduli is of the form

$$\text{Modulus (} 10^9 \text{ Pa)} = C_0 + C_1 \cdot T$$

where  $T$  is temperature in  $^{\circ}\text{C}$  and the coefficients  $C_0$  and  $C_1$  are given in Table II.

Figures 6 through 9 show bulk modulus, Young's modulus, shear modulus, and Poisson's ratio as functions of temperature. It is clear that the transition  $\zeta \rightarrow \zeta'$ , which occurs at  $190^{\circ}\text{C}$ , has a significant effect on these mechanical properties. Variations in the longitudinal velocity in the two  $\delta$ -phase specimens were as great as 5 pct, resulting in 10 pct moduli changes. This velocity change may have been caused by the presence of small internal cracks or by texture.

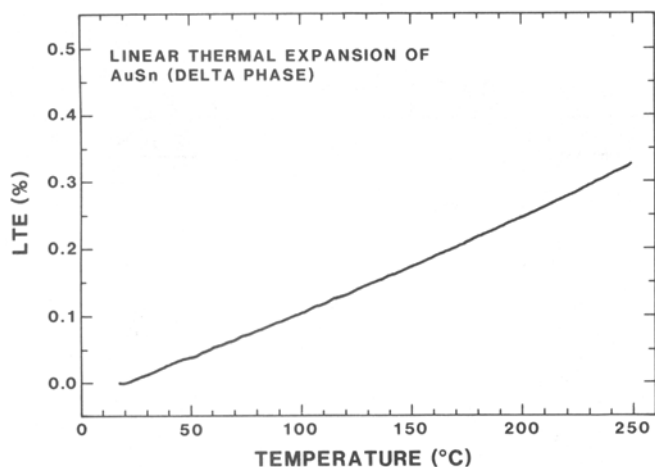


Fig. 3—Linear thermal expansion ( $\Delta L/L_0$  pct) of  $\delta$  phase vs temperature measured after a 5-day anneal at  $150^{\circ}\text{C}$ .

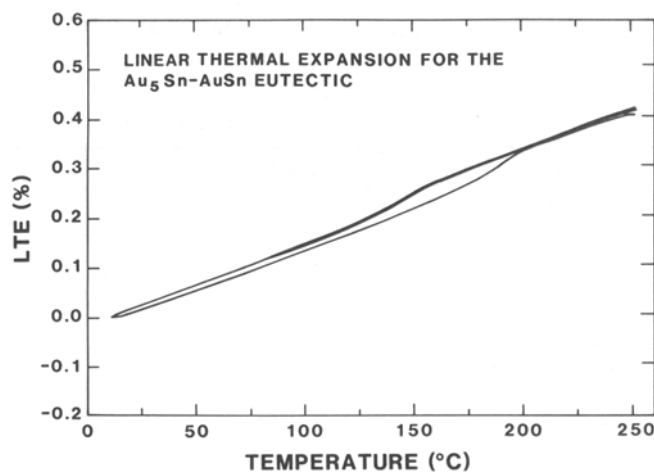


Fig. 4—Linear thermal expansion ( $\Delta L/L_0$  pct) of eutectic Au-Sn vs temperature measured after a 5-day anneal at  $150^{\circ}\text{C}$  and a 4-day anneal at  $250^{\circ}\text{C}$ . The lower curve is heating, and the upper curve is cooling.

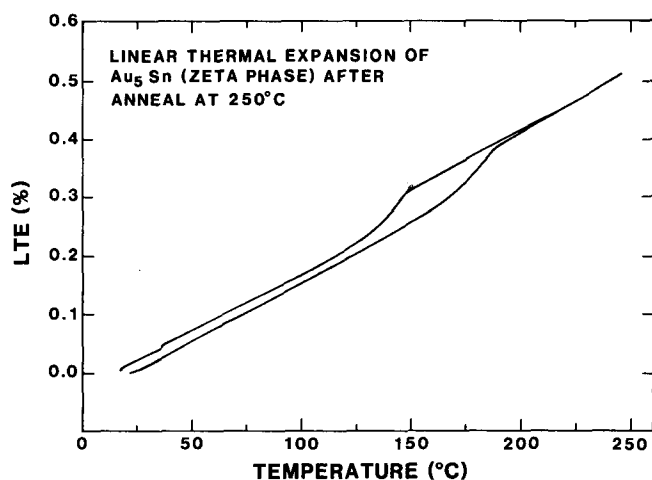


Fig. 5—Linear thermal expansion ( $\Delta L/L_0$  pct) of  $\zeta$  phase vs temperature measured after a 5-day anneal at 150 °C and an 8-day anneal at 250 °C. The lower curve is heating, and the upper curve is cooling.

#### IV. DISCUSSION

Parts joined by the eutectic alloy usually have gold films on their mating faces. When the eutectic melts, the gold films partially or entirely dissolve, depending on time and temperature. The amount of Au dissolved into the molten alloy determines the resulting joint composition. Hence, the expansion and resulting thermal stress in this joint would be bounded by the thermal behavior of the  $\zeta$ -phase and eutectic alloys. At first glance, the Au-Sn eutectic seems an unwise choice for a die attach or lid seal alloy, because it is composed of two intermetallic compounds and these materials are characteristically brittle and unforgiving. The  $\zeta \rightarrow \zeta'$  phase transformation entails a volume change that may induce cracking and loss of hermeticity. During the cooling stage of a given processing step, such as lid sealing, the phase transformation may not proceed to completion, and any residual  $\zeta$  phase could then slowly transform to  $\zeta'$  at any temperature less than 190 °C, including room temperature. Despite these problems, the alloy has been used for many years with little difficulty. At the time of Bernstein's thermal expansion measurements, the Au-Sn phase diagram showed no phase transformation;<sup>[10]</sup> thus, his ob-

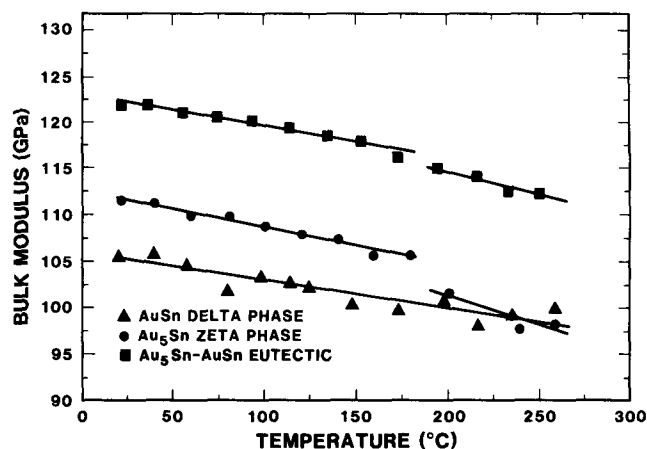


Fig. 6—Bulk modulus of  $\delta$ ,  $\zeta$ , and eutectic alloys vs temperature. All specimens were annealed for 5 days at 150 °C. The  $\zeta$  phase received an additional 8 days at 250 °C and the eutectic specimen an additional 4 days at 250 °C.

served dip was considered unusual. It is now recognized that the dip is associated with the phase transformation  $\zeta \rightarrow \zeta'$  at approximately 190 °C.

The heating and cooling behavior of the eutectic and  $\zeta$ -phase alloys shows effects of the transformation but not the dip observed by Bernstein. The present data suggest that the transformation  $\zeta \rightarrow \zeta'$  involves a volume contraction; this is also supported by the lattice parameter data given by Okamoto and Massalski.<sup>[7]</sup> Hysteresis in thermal expansion behavior due to phase transformations typically extends over a significant temperature range. For the eutectic and  $\zeta$ -phase alloys, this range spans approximately 40 °C. The expansion behavior of the  $\delta$  phase shows nearly linear behavior from room temperature to 250 °C.

All three moduli show behavioral change in the temperature range of 175 °C to 200 °C. These measurements were made under isothermal conditions and, thus, were not subject to thermal lag error. Had more measurements been taken near 190 °C, more abrupt changes would be anticipated in these properties. As expected, all moduli ( $B, E, G$ ) decrease with increasing temperature with  $B > E > G$ . Poisson's ratio shows a slight increase with temperature for all three alloys.

Table II. Coefficients  $C_0$ (GPa) and  $C_1$ (GPa/°C)

Sample	Coefficient	Young's Modulus	Shear Modulus	Poisson's Ratio	Bulk Modulus
$\delta$ phase	$C_0$	70.4	25.3	0.3	106.1
	$C_1$	-0.0(3)	-0.0(1)	0	-0.0(3)
Eutectic RT* to 190 °C	$C_0$	69.0	24.5	0.4	123.2
	$C_1$	-0.0(4)	-0.0(2)	0	-0.0(4)
Eutectic Above 190 °C	$C_0$	70.6	25.1	0.4	124.5
	$C_1$	-0.0(6)	-0.0(2)	0	-0.0(5)
$\zeta'$ phase RT to 190 °C	$C_0$	60.8	21.6	0.4	112.6
	$C_1$	-0.0(3)	-0.0(1)	0	-0.0(4)
$\zeta$ phase Above 190 °C	$C_0$	57.7	20.1	0.4	113.8
	$C_1$	-0.0(3)	-0.0(1)	0	-0.0(6)

\*RT = room temperature.

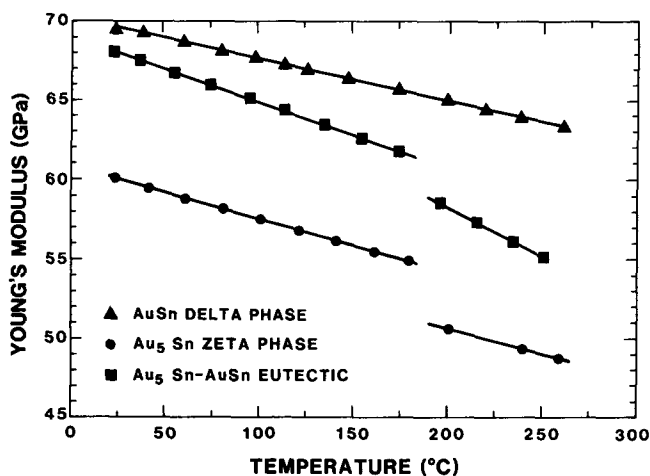


Fig. 7—Young's modulus of  $\delta$ ,  $\zeta$ , and eutectic alloys vs temperature. All specimens were annealed for 5 days at 150 °C. The  $\zeta$  phase received an additional 8 days at 250 °C and the eutectic specimen an additional 4 days at 250 °C.

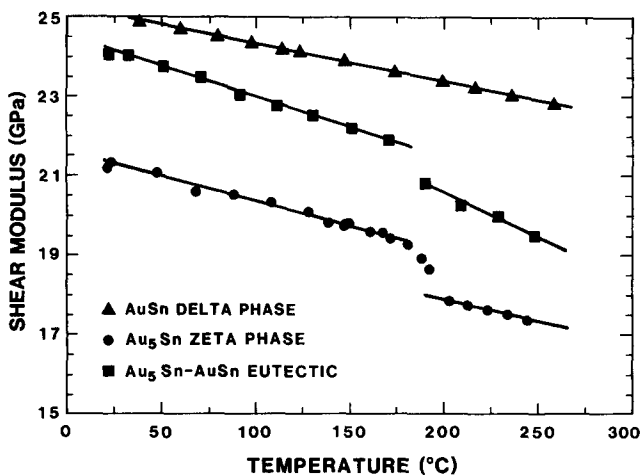


Fig. 8—Shear modulus of  $\delta$ ,  $\zeta$ , and eutectic alloys vs temperature. All specimens were annealed for 5 days at 150 °C. The  $\zeta$  phase received an additional 8 days at 250 °C and the eutectic specimen an additional 4 days at 250 °C.

## V. CONCLUSIONS

The Au-Sn eutectic alloy at 29 at. pct Sn and its two constituent phases,  $\zeta$  and  $\delta$ , were prepared by melting and solidifying pure Au and Sn. Following heat treatment, density, thermal expansion, and elastic moduli measurements were made on the three specimens. These data suggest that the order-disorder phase transformation,  $\zeta \rightarrow \zeta'$ , involves a volume contraction. Effects of

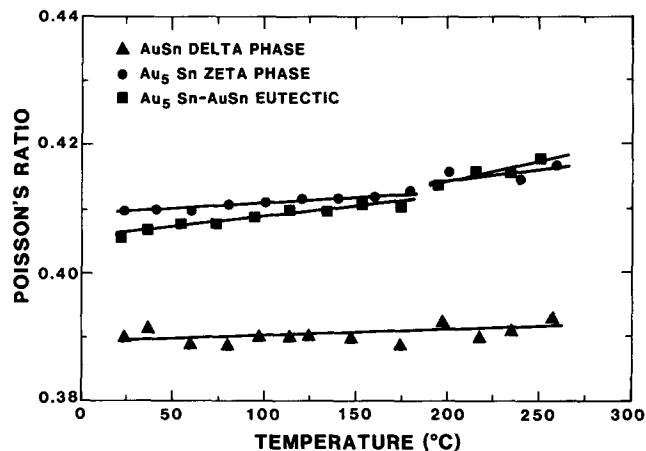


Fig. 9—Poisson's ratio of  $\delta$ ,  $\zeta$ , and eutectic alloys vs temperature. All specimens were annealed for 5 days at 150 °C. The  $\zeta$  phase received an additional 8 days at 250 °C and the eutectic specimen an additional 4 days at 250 °C.

this transformation could be seen near 190 °C (the transformation temperature) in both expansion and moduli measurements.

## ACKNOWLEDGMENTS

The authors are grateful to W.B. Chambers, O. Espinosa, F.A. Greulich, C.R. Hills, and W.R. Sorenson for laboratory analytical support. This work was performed at Sandia National Laboratories, supported by the United States Department of Energy under Contract No. DE-AC04-76DP00789.

## REFERENCES

1. L. Bernstein: *Semiconductor Products*, 1961, July, pp. 29-32.
2. L. Bernstein: *Semiconductor Products*, 1961, Aug., pp. 35-39.
3. D.D. Zimmerman: *Solid State Technol.*, 1972, Jan., pp. 44-46.
4. B.C. Giessen: *Z. Metallkd.*, 1968, vol. 59, pp. 805-09.
5. K.N. Ishihara, H. Gohchi, and P.H. Shingu: in *Undercooled Alloy Phases*, E.W. Collings and C.C. Koch, eds., TMS-AIME, Warrendale, PA, 1987, pp. 49-57.
6. K. Osada, S. Yamaguchi, and M. Hirabayashi: *Trans. Jpn. Inst. Met.*, 1974, vol. 15, pp. 256-60.
7. H. Okamoto and T.B. Massalski: *Phase Diagrams of Binary Gold Alloys*, ASM INTERNATIONAL, Metals Park, OH, 1987, pp. 278-88.
8. H.B. Huntington: in *Solid State Physics*, F. Seitz and D. Turnbull, eds., Academic Press, Inc., New York, NY, 1958, vol. 7, pp. 221-22.
9. J.H. Gieske and H.M. Frost: *Review of Progress in Quantitative Nondestructive Evaluation*, 1988, vol. 8, pp. 1709-16.
10. M. Hansen and K. Anderko: *Constitution of Binary Alloys*, McGraw-Hill, New York, NY, 1958, pp. 232-34.